FULL-SCALE FIRE RESISTANCE TESTING OF CONCRETE BEAMS REINFORCED WITH VARIOUS FRP REINFORCEMENT

K. PROTCHENKO[1], M. URBAŃSKI[2]

The widespread use of Fibre-Reinforced Polymers (FRP) reinforced concrete (RC) structural members is hindered by their low fire resistant characteristics, limiting their use to cases, where fire resistance is not a priority. Presented and discussed are experimental results pertaining to the flexural members subjected to heating and simultaneous loading. Solely non-metallic FRP bars: (i) Basalt FRP (BFRP), (ii) Hybrid FRP (HFRP) with carbon and basalt fibres and (ii) nano-Hybrid FRP (nHFRP) with modified epoxy resin, were used as internal reinforcement for beams. The destruction of the beams was caused in different ways, beams reinforced with BFRP bars were destroyed by reinforcement failure while those reinforced with hybrid FRP bars were destroyed by concrete crushing. The BFRP reinforced beams obtained a maximum temperature, measured directly on the bars, of *917°C*, compared to beams reinforced with hybrid FRP bars, where the temperature on the bars reached *400-550°C* at failure. Moreover, the highest registered ductility was obtained for BFRP reinforced beams as well, where the maximum deflections reached approximately *16 cm*.

Keywords: Fibre-Reinforced Polymers (FRP) bars, Hybrid FRP bars, FRP-RC beams, Fire resistance of FRP, Fire resistance of FRP-RC members

[1] MSc, Eng., Warsaw University of Technology, Faculty of Civil Engineering, Al. Armii Ludowej 16, 00-637 Warsaw, Poland, e-mail: k.protchenko@il.pw.edu.pl

[2] PhD., Eng., Warsaw University of Technology, Faculty of Civil Engineering, Al. Armii Ludowej 16, 00-637 Warsaw, Poland, e-mail: m.urbanski@il.pw.edu.pl

1. INTRODUCTION

Fibre-Reinforced Polymers (FRP) composite materials have the advantage of high strength and stiffness, as well as a low density and highly flexible tailoring [1]. Therefore, their use in the form of FRP bars as a replacement of conventional reinforcement for reinforced concrete (RC) structures has become attractive. In addition, these materials are unaffected by electrochemical deterioration, and are relatively resistant to corrosion, which can prevent to the deterioration of concrete and a loss of structural integrity [2-4].

One of the major issues that hinder the extensive use of FRP reinforced members is their low fire resistance, which is of high importance since building structures must satisfy the requirements of building codes, which relate to the behaviour of those structures in a fire. Fire ratings for buildings refer to the amount of time a structure can be exposed to fire before the structure collapses [5]. The relevant property of the FRP bars is not its flammability or reaction to fire, but rather its ability to continue to sustain loads in an environment of rapidly rising temperatures [6, 7].

FRP composites consist of unidirectional organic or inorganic fibres embedded in a thermosetting or thermoplastic polymer matrix [8]. The properties of FRP composites are dependent on the properties of their constituents and the relative proportions of the fibre, known as the fibre-volume ratio [9, 10]. The matrix can be seriously affected at elevated temperatures, therefore it is needed to examine the behaviour of bars subjected to fire exposure as well as structures reinforced with these materials [11]. Currently, the use of FRP reinforcement for RC structures is limited and only includes cases when fire resistance aspects are not particularly meaningful.

The failure of any FRP-RC element depends on three parameters that should be considered during the design of FRP-RC members under fire conditions: strength of FRP, maximum bar temperature, and the anchorage length that is not directly subjected to fire [12]

Hence, the fire resistance of FRP reinforcement is an important issue that needs a careful analysis before being implemented in RC structures, but the available data from standards are scarce. ACI committee ACI 440.1R-15 [13] describes the material characteristics needed to design the minimum reinforcement in the perspective of temperature and shrinkage thresholds. The Canadian code CAN/CSA S806-12, Annex R for slabs [14] provides a design procedure in a fire situation based on critical temperatures related to the FRP bars [15].

Additionally, a different mechanical behaviour of FRP bars makes designing structures with FRP reinforcement differ from conventional RC design. The progress in manufacturing technology

has introduced new types of FRP bars, and furthermore Hybrid FRP (HFRP) which allow one to adjust FRP characteristics to a specific design situation. HFRP bars contain several types of reinforcing constituents and/or several types of adhesive constituents in a matrix. Moreover, some authors suggest that hybridization of the constituents of FRP bars can prevent changes in their behaviour, making it semi-ductile instead of linear [2].

Furthermore there is an absence of recommendations on the use of HFRP bars in the available design codes and guides, as well as a lack of information, if the presence of other components, such as reinforcing fibres or a modification of matrix, can cause any difference on the overall behaviour of composites under fire exposure.

The behaviour of an individual RC structure containing several load-bearing elements subjected to elevated temperatures is a complex issue, which requires the nonlinear properties of the material and geometry to be examined [16]. Therefore, the tests on separate structural members which could be an effective starting point were conducted.

The purpose of the present study is to investigate experimentally the fire resistance of FRP-RC members under standard fire conditions, i.e. to conduct fire endurance tests. The experimental results related to the flexural performance of beams, before and during heating which were simultaneously loaded, were reported and discussed in this work.

2. EXPERIMENTAL PROGRAMME

The experimental work involved the preparation of *12* FRP-RC beams, solely non-metallic reinforcement was used. Six of the beams were tested under typical conditions in accordance with a standard heating curve ISO-834 (1990) [17]. The specimens were heated and simultaneously loaded in a four-point bending test by a sustained load until failure. The other six beams were used as reference specimens and were not subjected to temperature. The loading for the reference beams was increasing until failure.

A different configuration and type of bars was used for the tensile zone of beams. Therefore, beams were divided into two sets ("A" and "B") and two additional reference sets ("A-ref" and "B-ref") that were used for defining the ultimate strength capacity of the beams, measure deflections and to examine the character of the destruction of the beams.

2.1. MATERIALS UTILIZED IN THE WORK

2.1.1. CONCRETE

The beams were cured for a complete *28* day period in the lab before they were moved to the testing frame. The concrete mixture design was identical for all beams: a typical concrete mix *C40/45* was used. Ordinary Portland cement *CEM III/A*, ash, and crushed stone (silica) with a nominal maximum size of *16 mm* were used in the concrete mixes.

The concrete class was guaranteed by concrete manufacturing company. In addition, own laboratory tests were made on five cubic specimens. Table 1 presents the averages from test outcomes to confirm the concrete class of the beams.

Table 1. Mechanical Characteristics of Concrete used for the specimens

Period	Compressive strength, f_c	Tensile strength, f_{ct}	Modulus, E
28 days	48.75 MPa	4.23 MPa	37.83 GPa

2.1.2. REINFORCEMENT

The specimens were reinforced with different FRP bars, such as BFRP, HFRP and nano-Hybrid FRP (nHFRP) bars. Processing of hybrid bars is analogous to the process of producing of any other commercially available FRP bars, where a part of fibres is physically substituted with another fibre type. The selected volume fractions of carbon-to-basalt fibres for HFRP bars was assumed as *1:4* (i.e. *16%*) of carbon fibres, *64%* of basalt fibres and *20%* of epoxy resin).

For the nHFRP bars, apart fibres, the matrix was modified, a four-component *1300 System®* was added to the epoxy resin. A sol with nanosilica particles with a concentration of *25÷30%* by weight was used. The average diameter of particles was *24,7 nm*, containing two fractions: fine (*80%*) and coarse (*20%*). As it can be found in the literature, adding an appropriate sol of nanosilica particles to the matrix concentration can improve the chemical cohesion of nHFRP constituents and positively influence resistance to high temperatures [18-20].

After numerical and analytical considerations, HFRP and nHFRP bars were produced by external manufacturing company. BFRP bars were delivered by the same company in order to ensure the same basalt roving will be used with the same mechanical and physical properties. A detailed

overview on the elaboration of hybrid bars and their mechanical properties is provided in these companion papers [21-24].

The mean values of maximum force, F_u, limit stress, f_u, modulus of elasticity, E_1, and the limit strain, ε_u, for BFRP, HFRP and nHFRP bars were obtained experimentally from tensile tests at room temperature and are shown in Table 2.

Table 2. Mechanical properties of the FRP bars utilized in the tests

Type of bars	Maximum tensile force F_u	Tensile strength f_u	Tensile strain at rupture ε_u	Modulus of elasticity E_1
Type / Dia	[kN]	[MPa]	[%]	[GPa]
BFRP Ø6	37.07	1148.81	2.48	46. 47
BFRP Ø8	60.03	1103.30	2.52	43.87
HFRP Ø8	77.21	1277.92	1.73	73.89
nHFRP Ø8	71.28	1223.48	1.72	71.00
BFRP Ø14	179.26	1101.94	2.39	46.02
HFRP Ø14	206.57	1160.06	1.61	72.12
nHFRP Ø14	150.54	958.00	1.58	60.44

2.2. FRP-RC BEAMS PREPARATION

The FRP-RC beams had a rectangular section with dimensions *140 mm* wide, *260 mm* high and *3200 mm* long. The reinforcement in the compression zone and shear reinforcement (stirrups) were assumed to be consistent for all beams. The stirrups made of *6 mm* diameter BFRP bars have a spacing assumed to be *100 mm*. The mid part of the beam did not contain stirrups in order to simulate clear bending. The longitudinal top reinforcement is composed of two *8 mm* diameter BFRP bars. For the tensile reinforcement (bottom zone) different reinforcement types and amount were used, as shown on the Fig. 1. An additional explanation on the reinforcement is shown on the example of reinforcement configuration (Sample *H2Ø14*) in the Fig. 2. The clear cover, c_{nom}, was equal to *30 mm* from all sides for all tested specimens.
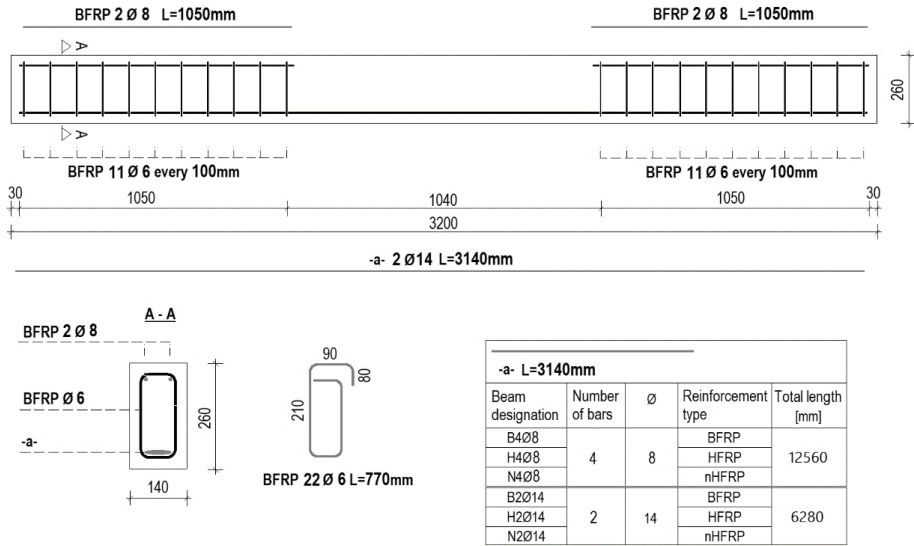
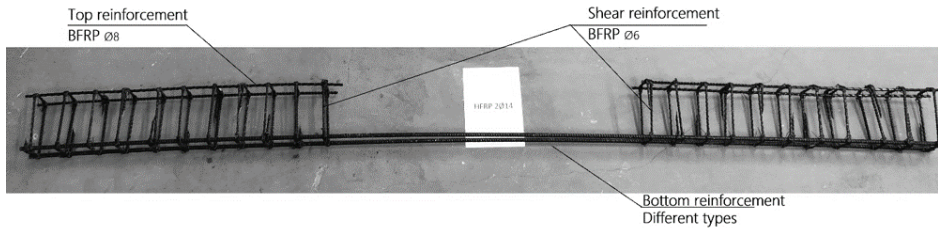Fig. 1. Reinforcement configuration of the beams.

Fig. 2. An example of reinforcement configuration - side view, *H2Ø14*

Depending on the tensile reinforcement, the beams were divided into sets, (i) Set A composed of three beams reinforced with four FRP bars of the diameter *8 mm* and (ii) Set B composed of three beams reinforced with two FRP bars of the diameter *14 mm*. The beams of sets A and B were preliminary loaded and unloaded with *50%* ultimate strength of beams before being heated. Six corresponding beams of Set A-ref and B-ref were used as reference beams and were loaded gradually until failure (without temperature).

The description for the specimen and loading is described in the Table 3.

Table 3. Loading and description of specimens

Set name	Beam designation	Reinforcement ratio	Reinforcement (tension zone)	Preliminary loaded (force) (50% of ultimate load, obtained with A-ref and B-ref)
		%	Number / Dia / Type	kN
A	B4Ø8	0.652	4 / 8 / BFRP	32
	H4Ø8		4 / 8 / HFRP	34
	N4Ø8		4 / 8 / nHFRP	40
B	B2Ø14	1.013	2 / 14 / BFRP	35
	H2Ø14		2 / 14 / HFRP	36
	N2Ø14		2 / 14 / nHFRP	45

Prior to casting, every specimen was instrumented with eight thermocouples in the concrete at different locations as well as on the bars to represent the temperature distribution during testing. The thermocouples were placed in the mid-part of the beam and near the furnace edges both inside and outside the beam.

Three dial gauges were applied on the top face to measure deflections. In addition, two dial gauges were added on the sides to measure possible beam extensions. Outputs were recorded every half second during the test. Fig. 3 shows the test setup of the beams and their instrumentation.

The process was as follows: at first beams were loaded by a sustained loading that corresponds to *50%* of their ultimate strength, as it is described in Table 3. Afterwards, the furnace was moved under the beam and moved into place (as described in Fig. 3 and Fig. 4). The beams were subjected to specific fire actions, i.e. the mid-section was heated from the bottom as well as from parts of both sides. The gaps between the interfaces of the beam and edges of the furnace were carefully insulated with ceramic and rock wool. The loading and heating were applied until failure of the beams. Fig. 4 shows the test setup during the heating phase.
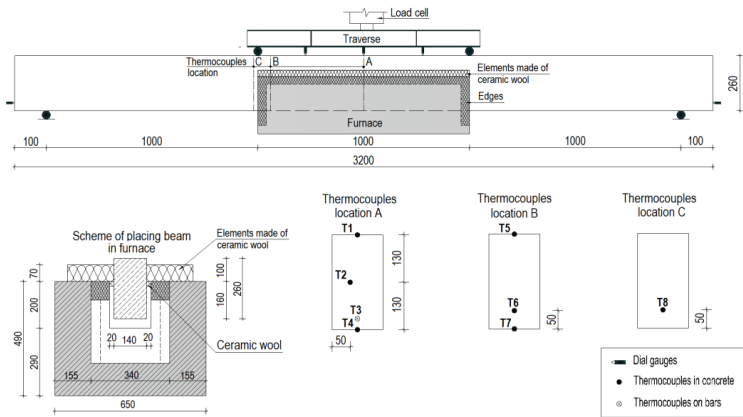
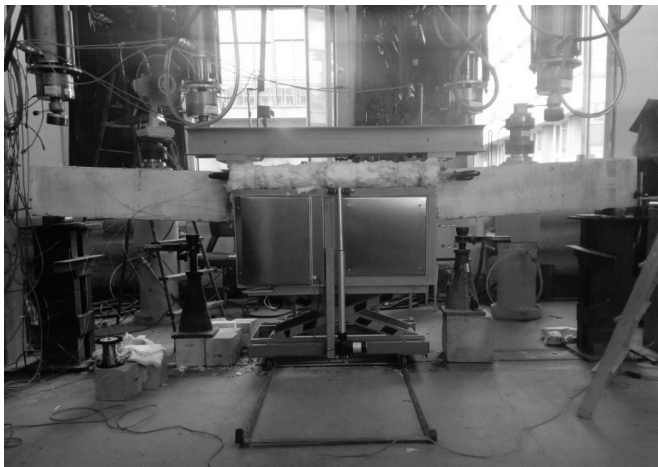Fig. 3. Test setup scheme and instrumentation of the beams

Fig. 4. Test setup of specimen, *B2Ø14 – Set B*, being heated and loaded simultaneously

3. RESULTS AND DISCUSSION

Unlike the reference specimens, which were destroyed due to concrete being crushed in the compression zone, the failure of beams from Sets A and B occurred in different ways and was dependant on the type of bottom reinforcement. Two beams reinforced with BFRP bars were destroyed due to failure of the reinforcement in the tension zone and four beams reinforced with

hybrid FRP bars failed because of concrete crushing. Fig. 5 represents the specimens failure for the beams *N2Ø14* and *B2Ø14* just after the furnace was removed. Figures 5 (a) and 5 (b) show that beams with hybrid and basalt reinforcement have different failure pattern.


<center>(a)</center> <center>(b)</center>
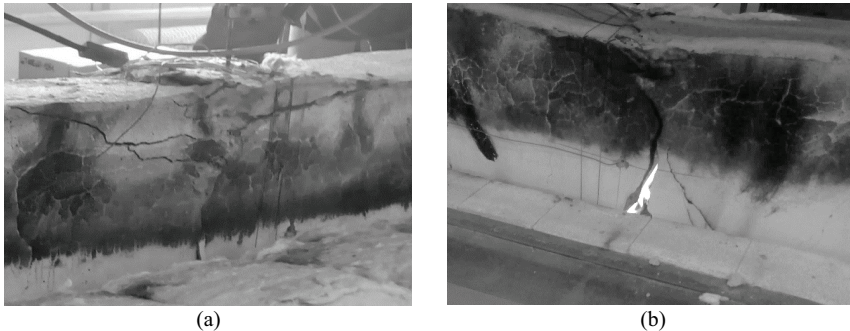
Fig. 5. Failure of the specimens: (a) *N2Ø14* (b) *B2Ø14*

As it can be seen on Fig. 6 (a) after the hybrid FRP bars were uncovered by removing the clear cover, which showed that the temperature caused a burning of the FRP bars. This resulted in the evaporation of the matrix in the middle of the bars. A major part of the fibres stayed in the same place and continued to sustain the load. Fig. 6 (b) shows four uncovered nHFRP bars after concrete crushing in the specimen *N4Ø8*, and Fig. 6 (c) represents the failure of two BFRP bars in the specimen *B2Ø14*.

<center>(a)</center>

<center>(b)   (c)</center>
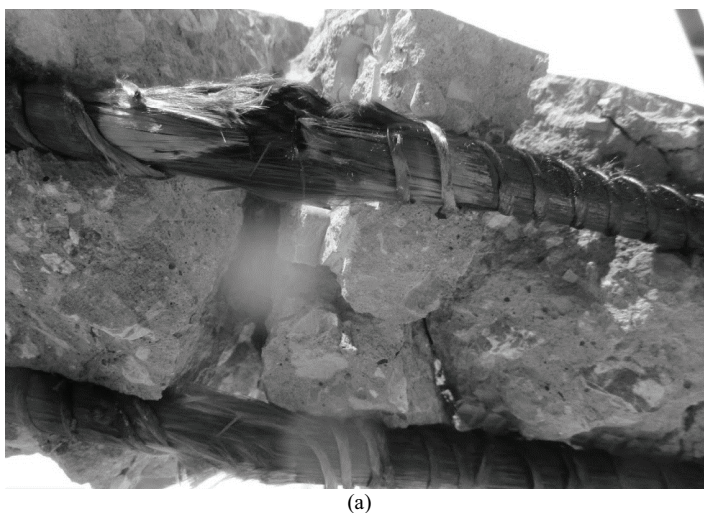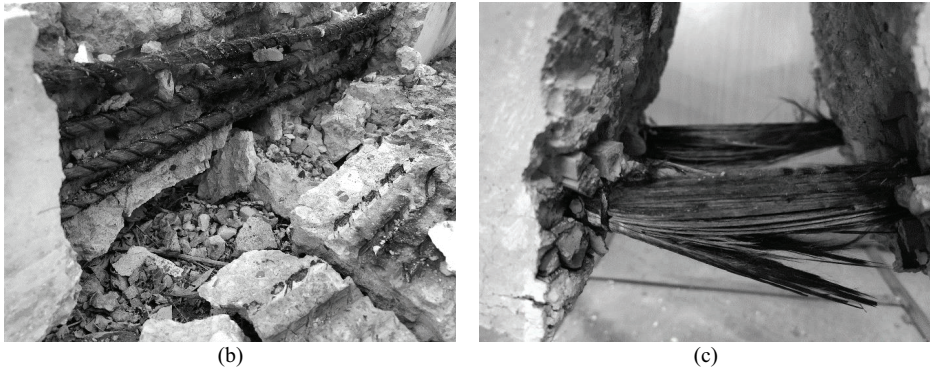
Fig. 6. Destruction of the beams: (a) HFRP bars after the matrix evaporated in specimen *H2Ø14*;
(b) uncovered nHFRP bars in beam *N4Ø8*; (c) BFRP bars after the failure in the beam *B2Ø14*

The temperature, however, caused de-bonding with concrete, completely separating the reinforcement with the concrete. The bars were disconnected with concrete mainly in the places were heating was applied, and it was common for all specimens. Fig. 7 (a) represents de-bonding of HFRP bars and concrete, and Fig.7 (b) shows the concrete surface after taking bars out.

<center>(a)   (b)</center>

Fig. 7. De-bonding of HFRP bars: (a) separated HFRP bars after being uncovered from concrete;
(b) concrete surface after taking the bars out.

In accordance with several studies, there are two critical temperature thresholds for bars that can be distinguished, the first one comes at an early stage causing interface cracking and de-bonding with concrete [25, 26]. The second threshold is not precisely known, but it leads to significant

reductions in strength capacity of bars and in turn a failure of the FRP-RC structures [27, 28]. The temperature for the second threshold, which was identified from other studies was in the range *200-500 ^0C* [29].

However, the temperatures observed with thermocouples in the present work was varying. In most of the cases, the destruction of beams occurred when the temperature on the bars was approximately *400-550 ^0C*. However, in the case of BFRP bars, the critical temperature, measured on the bars, was the highest one, *593 ^0C* for *B2Ø14* and *ca. 917 ^0C* for *B4Ø8*. Moreover, the distinctive fact for beams reinforced with BFRP bars is that the destruction was caused by the failure of the reinforcement. Fig.8 shows the example of temperature distribution for the specimens *H2Ø14* measured with thermocouples in two locations.
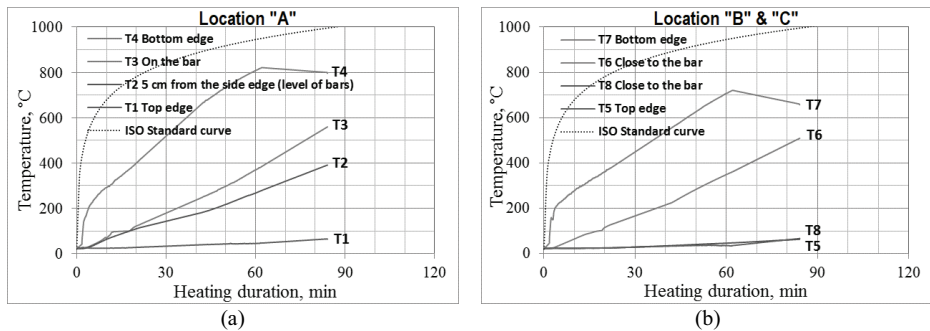

Fig. 8. Temperature distribution measured by thermocouples in three different locations for *H2Ø14*: (a) in the middle of the beam span, (b) inside and outside the edge of the furnace

The highest ductility, *heating time of 97 min*, was registered for the specimen *B2Ø14*. The deflections obtained for that beam were the greatest among all the beams; the central dial gauge showed *162 mm*. The specimen reinforced with four BFRP bars also showed the longest heating time in beams of Set A - *82 min*, which corresponded to *88 mm* deflections. Similar deflections were observed for beams of sets A and B reinforced with hybrid FRP bars. Fig. 9 describes the heating time - vertical deflection curves measured by three dial gauges during testing of Sets A and B.
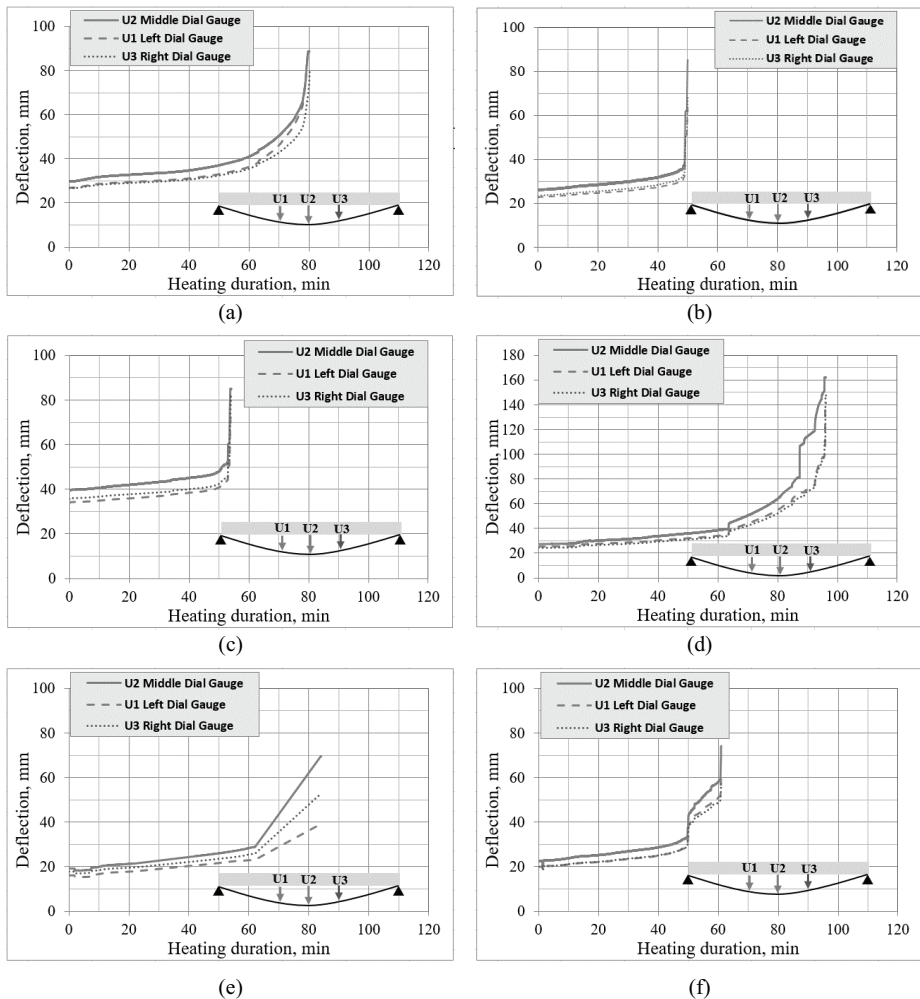
Figure 9. Heating duration - vertical deflections curves: (a) *B4Ø8* (b) *H4Ø8* (c) *N4Ø8* (d) *B2Ø14* (e) *H2Ø14* (f) *N2Ø14*

During standard fire resistance testing, the deflections measured for both sets (Set A and B) were greater than the deflections obtained for reference specimens (Set A-ref and Set B-ref), six times higher deflections were recorded for BFRP reinforced beams (for *B2Ø14*). However, it is worth mentioning that only gradual loading was applied for reference beams until 50% of ultimate load (shown in the Table 3), while for standard

fire resistance testing, the specimens were subjected to sustain loading and specific fire actions for longer time. The maximum deflections for beams obtained during fire resistance testing and deflections measured for reference beams are shown in the Table 4.

Table 4. Comparison of the maximum deflections for tested and reference beams

Beams loaded under fire conditions			Reference beams		
Set name	Beam designation	Deflections, mm	Set name	Beam designation	Deflections (measured at 50% of ultimate load), mm
A	*B4Ø8*	89	A-ref	*B4Ø8-ref*	32
	H4Ø8	85		*H4Ø8-ref*	30
	N4Ø8	84		*N4Ø8-ref*	32
B	*B2Ø14*	162	B-ref	*B2Ø14-ref*	27
	H2Ø14	70		*H2Ø14-ref*	17
	N2Ø14	75		*N2Ø14-ref*	22

The beam deflection for the same beams tested in normal temperatures depends on the stiffness of the bars used. Stiffness is the product of the elastic modulus and the moment of inertia. The larger bar diameter corresponds to the greater moment of inertia. The modulus of elasticity of the BFRP bars is lower than that of the HFRP and nHFRP bars. Hence, for similar diameters, the stiffness of the HFRP and nHFRP bars will be greater than the stiffness of the BFRP bars. Thus, for the same load, the deflection of beams with HFRP and nHFRP rebars will be smaller than those for beams reinforced with BFRP bars in normal temperatures.

During fire resistance testing, the deflection for the beams reinforced with BFRP bars were also greater for both sets A and B (as it can be seen from the Table 4 and Figure 9) correspondingly, the heating time of BFRP reinforced beams was longer. The higher deflections of BFRP reinforced beams can be explained by the mechanical properties of BFRP bars. Despite the fact, that the tensile strength of nHFRP and HFRP bars is higher comparing to BFRP bars, the modulus of elasticity of BFRP bars is smaller. Therefore, the deflections of BFRP reinforced beams were higher due to the stiffness of the bars.

The fact that beams reinforced with nHFRP bars failed faster than HFRP and BFRP reinforced beams might be considered as a result from an improper execution and incorrect redistribution of nanosilica particles in the nHFRP bars. The tests were carried out for a limited amount of reinforcement and bar diameters, the results will serve for identifying the key factors for further investigations.

3. CONCLUSIONS

The work was focused on the experimental testing of beams subjected to specific fire actions, which were simultaneously loaded by a sustained load that corresponds to *50%* of the ultimate strength capacity of the beams. The authors suggest that one of the reasons for the failure of the beams is the degradation of the bond between FRP bars and concrete caused by the incompatible coefficients of thermal expansion of the materials.

Corresponding reference beams were destroyed by concrete crushing, however beams that were heated and loaded failed in different ways; beams reinforced with BFRP bars were destroyed by reinforcement failure, while the beams reinforced with hybrid FRP bars were destroyed by concrete crushing. After the hybrid FRP bars were uncovered by removing the clear cover of concrete, it was visible that the matrix in the middle of the bars has been disappeared, however, a large part of the basalt and carbon fibres remained in the same place and continued to withstand the load.

The highest temperature and the longest period of heating was achieved by beams reinforced with BFRP bars in comparison to beams reinforced with hybrid FRP bars of the same sets. The duration of the heating phase for sample *B4Ø8* was approximately *82 min.*, deflections were *88 mm*, and the temperature on the bars, was *917 ºC*. The fire resistance for beams reinforced with HFRP and nHFRP bars showed similar results for both sets. However, for the sample *B2Ø14* even better results has been recorded, *97 minutes* and the temperature of *593 ºC* and *162 mm* deflections were obtained for the sample before destruction.

The results showed that the fire resistance of FRP-RC members was varying depending on the type of reinforcement used, that can indicate on a significant role of the composition of bars on FRP-RC performance at elevated temperatures.

REFERENCES

1. K. Nguyen, J.P. Tran, T. Ngo, P. Tran, P. Mendis, "Experimental and computational investigations on fire resistance of GFRP composite for building façade", Composites Part B: Engineering 62: 218–229, 2014. https://doi.org/10.1016/j.compositesb.2014.02.010

2. T.A. Elsayed, A.A. Elhefnawy, A.A. Eldaly, G.M. Ghanem, "Hybrid fiber reinforced polymers rebars", Journal of Advanced Materials 43: 65-75, 2011.

3. A. Nanni, A. De Luca, H. Jawaheri Zadeh, "Reinforced concrete with FRP bars: Mechanics and design", CRC Press, Boca Raton, FL, 2014.

4. E. D. Szmigiera, M. Urbański, and K. Protchenko, "Strength Performance of Concrete Beams Reinforced with BFRP Bars," in International Congress on Polymers in Concrete (ICPIC 2018) : Polymers for Resilient and Sustainable Concrete Infrastructure, 2018, pp. 667–674. http://doi.org/10.1007/978-3-319-78175-4_85

5. R. Kowalski, M.J. Głowacki, M. Abramowicz, "Premature destruction of two-span RC beams exposed to high temperature caused by a redistribution of shear forces", Journal of Civil Engineering and Manufacturing 22(8), 1–9, 2016. https://doi.org/10.1260/2040-2317.6.1.49

6. A. Abbasi, P. Hogg, "Temperature and environmental effects on glass fibre rebar: Modulus, strength and interfacial bond strength with concrete", Composites Part B: Engineering36: 394-404, 2005. https://doi.org/10.1016/j.compositesb.2005.01.006

7. K. Protchenko and E. D. Szmigiera, "Post-Fire Characteristics of Concrete Beams Reinforced with Hybrid FRP Bars," Materials, vol. 13, no. 5, pp. 1–15, 2020. http://doi.org/10.3390/ma13051248

8. R. Hamad, M.A. Megat Johari, R. Haddad, "Effects of Bars Slippage on the Pre- and Post-Heating Flexural Behavior of FRP Reinforced Concrete Beams: Experimental and Theoretical Investigations", International Journal of Civil Engineering and Technologes 10: 574-602, 2019.

9. D.S. Ellis, H. Tabatabai, A. Nabizadeh, "Residual Tensile Strength and Bond Properties of GFRP Bars after Exposure to Elevated Temperatures", Materials 11: 346, 2018. https://doi.org/10.3390/ma11030346

10. K. Protchenko, M. Włodarczyk, and E. D. Szmigiera, "Investigation of Behavior of Reinforced Concrete Elements Strengthened with FRP," Procedia Engineering, vol. 111, pp. 679–686, 2015. http://doi.org/10.1016/j.proeng.2015.07.132

11. K. Protchenko, E. D. Szmigiera, M. Urbański, A. Garbacz, P. L. Narloch, and P. Lesniak, "State-of-the-Art on Fire Resistance Aspects of FRP Reinforcing Bars," IOP Conference Series: Materials Science and Engineering, vol. 661, pp. 1–8, 2019. http://doi.org/10.1088/1757-899X/661/1/012081

12. E. Nigro, G. Cefarelli, A. Bilotta, G. Manfredi, E. Cosenza, "Fire resistance of concrete slabs reinforced with FRP bars Part I: Experimental investigations on mechanical behaviour", Composites: Part B: Engineering Vol. 42: 1739–1750, 2011. https://doi.org/10.1016/j.compositesb.2011.02.025

13. ACI. Guide for the design and construction of concrete reinforced with FRP Bars. ACI 440.1R-15. Farmington Hills, MI: American Concrete Institute; 2015.

14. CSA. Design and construction of building structures with fibre-reinforced polymers. CAN/CSA S806-12, Canadian Standards Association, 2012, Reaffirmed in 2017, 206 pages.

15. E. Nigro, G. Cefarelli, A. Bilotta, G. Manfredi, E. Cosenza, "Fire resistance of concrete slabs reinforced with FRP bars part II: experimental results and numerical simulations on the thermal field", Composites Part B: Engineering, 42 (6): 1751–1763, 2011. https://doi.org/10.1016/j.compositesb.2011.02.026

16. H. Hajiloo, M. Green, M. Noël, N. Benichou, M.A. Sultan, "Fire Tests on Full-Scale FRP Reinforced Concrete Slabs", Journal of Composite Structures 179: 705-719, 2017. https://doi.org/10.1016/j.compstruct.2017.07.060

17. ISO 834-1, Fire Resistance Tests – Elements of Buildings Construction, Part-1 General Requirements, International Organization for Standardization, Switzerland, 1999.

18. L.P. Gao, D.Y. Wang, Y.Z. Wang, J.S. Wang, B. Yang, "A flame-retardant epoxy resin based on a reactive phosphorus-containing monomer of DODPP and its thermal and flameretardant properties", Polym Degrad Stabil 93: 308–1315, 2008.

19. Y.X. Zhou, P.X. Wu, Z.Y. Cheng, J. Ingram, S. Jeelani, "Improvement in electrical, thermal and mechanical properties of epoxy by filling carbon nanotube", Express Pol Let 2: 40-48, 2008. https://doi.org/10.3144/expresspolymlett.2008.6

20. S. Nazare, B.K. Kandola, A.R. Horrocks, "Flame-retardant unsaturated polyester resin incorporating nanoclays", Polymers for Advanced Technologies, 17: 294–303, 2006. https://doi.org/10.1002/pat.687

21. A. Garbacz, E.D. Szmigiera, K. Protchenko, M. Urbański, "On Mechanical Characteristics of HFRP Bars with Various Types of Hybridization", In M. M. Reda Taha, U. Girum, & G. Moneeb, M. M. Reda Taha, U. Girum, & G. Moneeb (Eds.), International Congress on Polymers in Concrete (ICPIC 2018) : Polymers for Resilient and Sustainable Concrete Infrastructure. Washington: Springer, 653–658, 2018. http://doi.org/10.1007/978-3-319-78175-4_83

22. K. Protchenko, E.D. Szmigiera, M. Urbański, A. Garbacz, "Development of Innovative HFRP Bars", MATEC Web of Conferences 196: 1–6, 2018. http://doi.org/10.1051/matecconf/201819604087

23. E.D. Szmigiera, K. Protchenko, M. Urbański, A. Garbacz, "Mechanical Properties of Hybrid FRP Bars and Nano-Hybrid FRP Bars", Archives of Civil Engineering 65(1): 97–110, 2019. http://doi.org/10.2478/ace-2019-0007

24. K. Protchenko, J. Dobosz, M. Urbański, A. Garbacz, "Wpływ substytucji włókien bazaltowych przez włókna węglowe na właściwości mechaniczne prętów B/CFRP (HFRP)" [EN: Influence of the substitution of basalt fibres by carbon fibres on the mechanical behavior of B/CFRP (HFRP) bars]. Czasopismo Inżynierii Lądowej, Środowiska i Architektury, JCEEA 63, 1/1:149–156, 2016.

25. A. Abbasi, P. Hogg, "Fire Testing of Concrete Beams With Fibre Reinforced Plastic Rebar", Composites Part A: Applied Sciences and Manufacturing 37(8):1142-1150, 2006. https://doi.org/10.1016/j.compositesa.2005.05.029

26. A. Nadjai, D. Talamona, F. Ali, "Fire Performance of Concrete Beams Reinforced with FRP Bars", In: Proceedings of the International Symposium on Bond Behaviour of FRP in Structures (BBFS) 401-410, 2005.

27. E. Nigro, G. Cefarelli, A. Bilotta, G. Manfredi, E. Cosenza, "Performance under Fire Situations of Concrete Members Reinforced with FRP Rods: Bond Models and Design Nomograms", Journal of Composites for Construction 16(4): 395–406, 2012. https://ascelibrary.org/doi/abs/10.1061/(ASCE)CC.1943-5614.0000279

28. M. Rafi, A. Nadjai, F. Ali, P. O'Hare, "Evaluation of Thermal Resistance of FRP Reinforced Concrete Beams in Fire", Journal of Structural Fire Engineering 2(2): 91 –107, 2011. http://doi.org/10.1260/2040-2317.2.2.91

29. X. Wang, X. Zha, "Experimental Research on Mechanical Behavior of GFRP Bars under High Temperature", Applied Mechanics and Materials 71-78: 3591-3594, 2011.

LIST OF FIGURES AND TABLES:

Rys. 8. Rozkład temperatur mierzonych termoparami w wybranych punktach pomiarowych w trzech przekrojach belki *H2Ø14 (a) w środku belki (b) w przekrojach w środku i na zewnątrz blisko krawędzi pieca*

Fig. 9. Heating duration - vertical deflections curves: (a) *B4Ø8* (b) *H4Ø8* (c) *N4Ø8* (d) *B2Ø14* (e) *H2Ø14* (f) *N2Ø14*

Rys. 9. Zależność czas ogrzewania – ugięcia belek: (a) *B4Ø8* (b) *H4Ø8* (c) *N4Ø8* (d) *B2Ø14* (e) *H2Ø14* (f) *N2Ø14*

Tab. 1. Mechanical characteristics of concrete used for the specimens

Tab. 1. Cechy mechaniczne betonu badanych belek

Tab. 2. Mechanical properties of the FRP bars utilized in the tests

Tab. 2. Cechy mechaniczne zbrojenia FRP badanych belek

Tab. 3. Loading and description of specimens

Tab. 3. Oznaczenie i obciążenia badanych belek

Tab. 4. Comparison of the maximum deflections for tested and reference beams

Tab. 4. Porównanie maksymalnych ugięć badanych belek i referencyjnych

OGNIOODPORNOŚĆ PEŁNOWYMIAROWYCH BELEK BETONOWYCH ZBROJONYCH PRĘTAMI FRP O ZRÓŻNICOWANYM SKŁADZIE

STRESZCZENIE:

Degradacja nośności zbrojenia konstrukcji w postaci prętów FRP (ang. Fibre-Reinforced Polymers) może być spowodowane kilkoma czynnikami, do których należą: rodzaje włókien, osnowy (matrycy), ich objętościowy udział, sposób wytwarzania, jakość składników prętów. Jednakże głównym czynnikiem jest przede wszystkim wpływ temperatury w zbrojeniu FRP, występujący w trakcie oddziaływania warunków pożarowych. Zjawisko redukcji nośności konstrukcji i przyczepności zbrojenia do betonu pojawia się, gdy temperatura prętów FRP zbliża się do temperatury zeszklenia Tg osnowy (matrycy), której wartość zależy od rodzaju żywicy. Jednym z rozwiązań w tym zakresie jest zastosowanie większej otuliny lub zastosowanie dodatkowego systemu ochrony przeciwpożarowej.

Jednak obecnie dostępne dane na temat zachowania elementów betonowych zbrojonych FRP w warunkach pożarowych, są ograniczone, szczególnie w odniesieniu do nośności belek po poddaniu ich oddziaływaniu wysokich temperatur. Dlatego odporność ogniowa elementów betonowych zbrojonych FRP jest jednym z podstawowych czynników, które utrudniają powszechne stosowanie tych materiałów jako alternatywy dla zbrojenia stalowego.

W artykule opisano zachowanie się belek betonowych, zbrojonych prętami FRP wyprodukowanych na bazie włókien bazaltowych i węglowych, poddawanych testom odporności ogniowej. Badania belek narażonych na wysokie temperatury, przeprowadzono według scenariusz pożaru umownego zgodnie z krzywą standardową ISO-834 [13], [29]. Ponieważ głównym celem było zbadanie wpływu rodzaju zbrojenia FRP na odporność ogniową belek, zastosowano różne

rodzaje prętów w strefie rozciągania (dolna część belek): (i) zbrojenie na bazie włókien bazaltowych BFRP (ang. Basalt FRP), (ii) hybrydowe zbrojenie HFRP (ang. Hybrid FRP) z włóknami węglowymi i bazaltowymi oraz (ii) nano-hybrydowymi prętami nHFRP (ang. nano-Hybrid FRP) ze zmodyfikowaną żywicą epoksydową. Ponadto, badane elementy charakteryzowały się zmiennym stopniem zbrojenia, w celu określenia wpływu średnicy i liczby prętów na nośność belek podczas i po oddziaływaniu wysokich temperatur.

Przed betonowaniem wewnątrz badanych belek, w wybranych miejscach przekroju zainstalowano termopary w celu monitorowania temperatury prętów i betonu podczas oddziaływania pożaru. W każdej belce znajdowało się osiem termopar. Rozmieszczono je w środku rozpiętości elementu, a także w 2 przekrojach w pobliżu krawędzi pieca (wewnątrz i na zewnątrz pieca) co pozwoliło na określenie zmiany temperatury wzdłuż ogrzewanego odcinka, na całej wysokości belki.

W pierwszym etapie badań belki były stopniowo obciążane do 50% ich nośności, aby uzyskać realistyczną sytuację, np. występowanie rys (wartości otrzymano z próbek referencyjnych - bez wpływu temperatury). Następnie próbki poddano ogrzewaniu w środkowej części belek, od dołu i z boku, obciążenie pozostawało na tym samym poziomie. Belki ogrzewano aż do utraty nośności.

Mechanizm utraty nośności zależał od rodzaju zbrojenia rozciąganego. Belki zbrojone prętami BFRP ulegały awarii w strefie rozciągania, a utrata nośności belek zbrojonych prętami HFRP następowała na skutek skruszenia betonu w strefie ściskanej. Najwyższą temperaturę i najdłuższy okres nagrzewania uzyskano dla belek zbrojonych prętami BFRP w porównaniu do belek zbrojonych hybrydowymi prętami HFRP. Czas trwania fazy grzewczej dla belki zbrojonej czterema prętami BFRP o średnicy 8 mm wynosił około *82 min*., ugięcie osiągnęło wartość *88 mm*, a temperatura prętów rozciąganych wyniosła około *917 ºC*. Całkowita odporność ogniowa dla belek zbrojonych prętami HFRP i nHFRP była podobna.

Wyniki wykazały, że odporność ogniowa elementów zbrojonych prętami FRP różniła się w zależności od rodzaju zastosowanego zbrojenia, co może wskazywać, że skład prętów ma znaczący wpływ na zachowanie elementów zbrojonych FRP w podwyższonych temperaturach.